Chapter 12

Structural Enzymology of Aromatic Polyketide Synthase

Tyler Paz Korman, Brian Douglas Ames, and Shiou-Chuan Tsai

Departments of Molecular Biology and Biochemistry and Department of Chemistry, University of California, Irvine, CA 92697–3900

The type II (aromatic) polyketide synthase biosynthesizes many important antibiotic and anticancer polyketides in bacteria and fungi. Similar to the type II fatty acid synthase, the aromatic PKS carries out a series of reactions catalyzed by individual soluble enzymes, each of which are encoded by a discrete gene. The growing polyketide intermediates are transported between the enzymes attached to the acyl carrier protein through a thioester linkage. Using X-ray crystallography and NMR, enzyme structures from the actinorhodin and tetracenomycin PKSs have been solved. The structure of the individual PKS enzymes reveal key molecular features that help explain the observed substrate specificity, enzyme mechanism and protein-protein interactions. These structures are also a valuable resource to guide combinatorial biosynthesis of polyketide natural products.

In Polyketides; Rimando, Agnes M., et al.;
ACS Symposium Series; American Chemical Society: Washington, DC, 2007.

There are at least three characterized, architecturally different types of PKSs, although with better detection methods, the structural diversity of PKSs continues to increase (1). The focus of this chapter is the aromatic polyketide synthase (also called "Type II PKS") that biosynthesizes aromatic polyketides (Figure. 1), natural products that show an enormously rich and varied range of bioactivities. Examples include antibiotics (such as tetracyclines (2), tetracenomycin (3) and actinorhodin (4)), anticancer agents (such as resistomycin (5), doxorubicin (6) and mithramycin (7)), anti-fungals (such as pradimicin (8)) and anti-HIV therapeutics (such as rubromycin (9) and griseorhodin (10)) (11) (Figure 1). Despite extensive efforts to obtain polyketides synthetically due to their widespread medical applications, many aromatic polyketides have proven to be difficult to obtain via organic synthesis (12-14). By comparison, the biosynthesis of polyketides by polyketide synthase (PKS) offers a more economic and technically simpler protocol. By transforming the PKS gene into a bacterial host system followed by industrial fermentation, kilogram quantities of polyketides are routinely produced overnight (15). As a result, there is great interest in developing biosynthetic systems for the production of medically important polyketides.

The Molecular Logic of Aromatic PKS

The aromatic PKSs are comprised of 5-10 distinct enzymes whose active sites are used iteratively. Past molecular genetic studies in the groups of Hopwood (16), Hutchinson (17), Floss (18), Khosla (19), Robinson (20) and Salas (21) have established the current mechanism for a typical aromatic PKS (Fig. 2, the actinorhodin PKS): (1) Chain initiation: acyl carrier protein (ACP) primed by malonyl-CoA:ACP transacylase (MAT) (the involvement of MAT is an unresolved issue (22)); (2) Iterative chain elongation by the ketosynthase (KS) / chain length factor (CLF) heterodimer; (3) First-ring cyclization, either uncatalyzed or may involve enzyme domains; (4) Chain reduction by ketoreductase (KR); (5) First-ring aromatization by aromatase /cyclase (ARO/CYC); (6) Subsequent cyclization by the same or different ARO/CYCs. During each step, chain transfer between different catalytic domains is mediated by the phosphopentetheinyl group (PPT) covalently attached to a serine of ACP.

The advancement of PKS genetics has led to the development of a set of design rules for the rational manipulation of chain synthesis, reduction of keto groups and early cyclization steps (Figure 3): (1) The aromatic polyketide KR has a high specificity for the C9-carbonyl group (23). The C9-specificity is demonstrated by the product outcome during the biosyntheses of actinorhodin (4), doxorubicin (24), R1128 (25) and enterocin (26,27). In special cases, a highly specific reduction at other positions has also been observed (26,28). The structural basis this highly regio-specific behavior of KR is not well understood

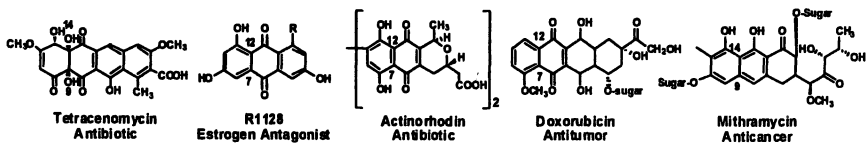

Figure 1. Representative Aromatic Polyketides that are numbered with the first ring cyclization specificity.

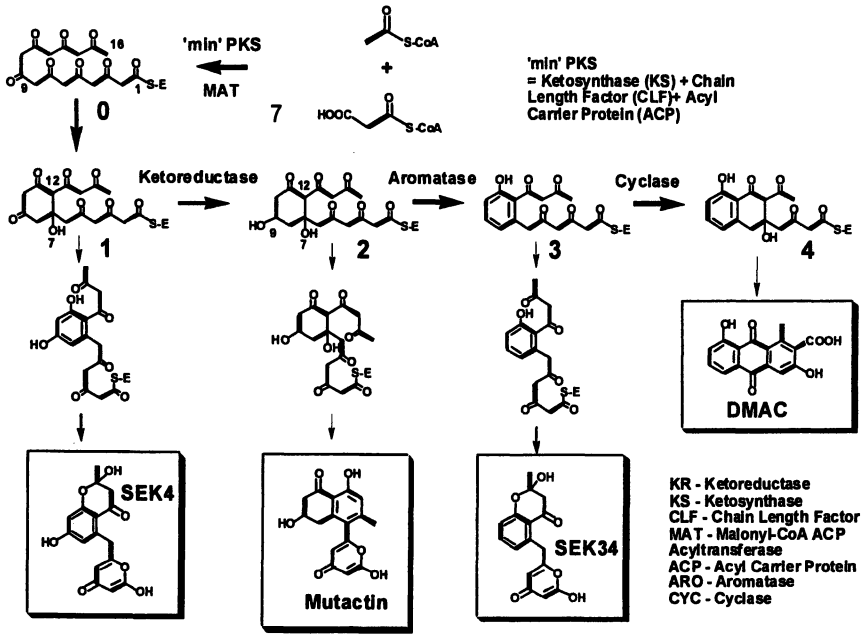

Figure 2. The Biosynthetic Pathway of Actinorhodin PKS

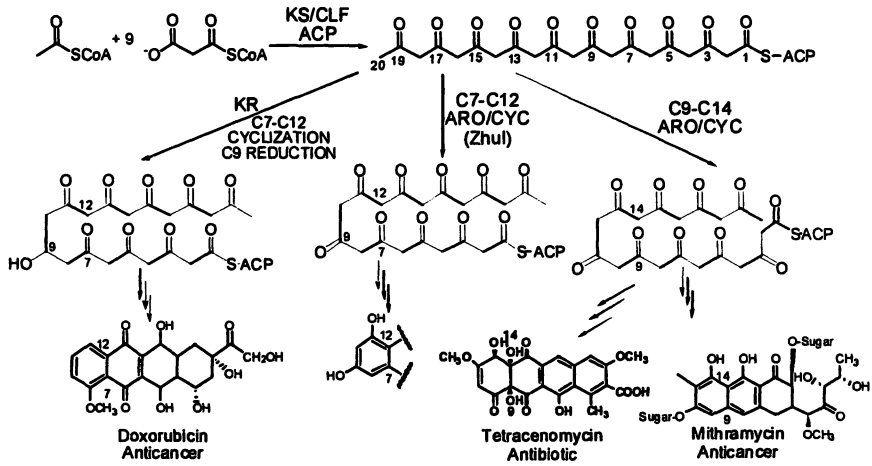

Figure 3. From the same polyketide chain, different cyclization patterns diversify polyketide products

(29). (2) The inclusion of KR often results in products that are cyclized at the C7-C12 positions (28,30), whereas the inclusion of a mono-domain ARO (in the absence of KR) often results in products that are cyclized at the C9-C14 positions (30,31) (Figure 3).

The above molecular rules have been used to rationally design polyketide products. Genetically engineered *Streptomyces* strains have produced new polyketides by expression of combinations of appropriate enzymatic subunits from naturally occurring polyketide synthase (the "mix and match" approach). These experiments have successfully created many novel polyketides (28,31-37) giving rise to > 100 new polyketides (37). The evidence cited above has led researchers in the field to appreciate that the large diversity of naturally occurring polyketides is a result of the controlled variation in chain length, a specific choice of building blocks and by differential chain modifications that are mediated by PKSs. The argument for the success of engineered biosynthsis is that natural selection process may have been very effective in identifying antibacterial polyketides due to the pressure of competition (38), but likely has not resulted in the selection of compounds with different pharmacologic activities. Therefore, the potential for development of new pharmaceutical based on bioengineering of novel polyketides is enormous.

A Summary of Aromatic PKS Structural work

Despite the advances cited above, random domain shuffling often results in complete inactivation of PKSs. For example, Burson and Khosla demonstrated that 90% of the shuffled KS/CLF domains resulted in the loss of activity (39). Further, because of our incomplete understanding of the mechanisms and specificities of individual enzymes, as well as the influence of protein-protein interactions in PKSs, many potential manipulations such as the rational control of cyclization patterns, are currently not available, (40). This lack of understanding about the structure-function relationship between PKS enzymes has recently been highlighted as a problem by Staunton and Weissman in the millennium PKS review (40). An important step toward remedying this limitation is to solve the crystal structures of individual PKS domains and then to use this knowledge to study the structure-function relationship of PKSs. Currently, crystal structures of the *S. coelicolor* MAT (41), the actinorhodin KS/CLF (42), the priming KS of R1128 (43), aclacinomycin-10-hydroxylase (44) and the actinorhodin oxygenase (45) have been solved. Several crystal structures of fatty acid synthase domains have also been solved (46,47), including the fatty acid MAT (48), ACP (49), KSs (50-52), KRs (46,53,54), enoylreductase (55-57) and dehydratases (58). In addition, the NMR structure of two polyketide ACP structures have been solved (59,60). Further, two cyclase structures, tcmI (61) and SnoaL (62), have been reported. These two cyclases catalyze the cyclization of the last ring during the biosyntheses of tetracenomycin and nogalamycin, respectively. They bear no sequence homology to the ARO/CYCs that promote the first and second ring formation (Figure 2). The structure-function relationship of the aromatic PKS domains help elucidate important molecular features such as chain length control, stereo- and regio-selectivity of KR, as well as the cyclization specificity of ARO/CYC. As a result, there remains a need for the crystal structures of polyketide KR and ARO/CYC. In this chapter, we will report our recent crystal structure solution of the actinorhodin KR, tetracenomycin ARO/CYC, as well as structure-based engineering of the actinorhodin KS/CLF.

Structure-Based Bioengineering of KS/CLF

The crystal structure of actinorhodin KS/CLF (which synthesizes a 16C chain) revealed an 18 Å long channel that starts with a conserved cysteine in the KS active site and spans across the KS-CLF dimer interface (Figure 4) (42). Residues lining the sides of the channel from both the KS and the CLF subunits are also well conserved. Sequence alignments of CLF subunits revealed that this

Publication Date: January 11, 2007 | doi: 10.1021/bk-2007-0955.ch012

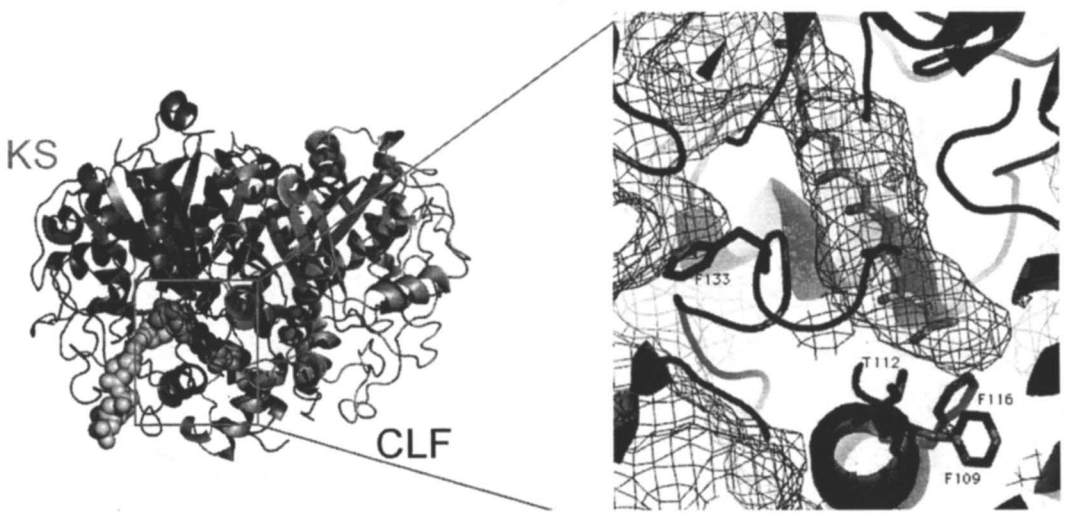

Figure 4. The Crystal structure of the actinorhodin KS/CLF, which catalyzes the formation of polyketide products with a 16-carbon backbone. The substrate binding channel is enlarged in the right panel. F109', T112' and F116' of CLF are located at the bottom of the substrate channel.

In Polyketides; Rimando, Agnes M., et al.;
ACS Symposium Series; American Chemical Society: Washington, DC, 2007.

region is highly conserved, except for residues 109, 112, 116, and 133 (*act* CLF numbering). The terminal wall of this channel is capped by a helix-turn-loop in the CLF, where F109', T112' and F116' are located. Remarkably, as chain length specificity increases from C_{16} to C_{24}, these four residues are replaced with less bulky amino acids. We hypothesize that these residues determine chain length. Therefore we constructed mutants of the *act* CLF bearing large-to-small changes at these positions using site-directed mutagenesis (Figure 4). The strain containing the wild-type *act* KS/CLF produced the expected 3,8-dihydroxy-1-methylanthraquinone-2-carboxylic acid (DMAC). Replacing the *act* KS/CLF with wild-type tetracenomycin (*tcm*) KS/CLF (a decaketide synthase) yielded RM20b as the major product. Significantly, >65% of the polyketide products of the double mutant F109A/F116A were decaketides. Triple mutations (F109A/T112A/F116A) did not alter the specificity further. The purified mutant actinorhodin KS/CLFs *in vitro* showed that F116A was sufficient to increase the levels of decaketides to 64% of the total polyketides, while the F109A/F116A double mutant synthesized decaketides as >95% of the total polyketides.

To probe the roles of the corresponding residues in a decaketide CLF, small-to-large mutations at G116 and M120 (*tcm* CLF numbering) were introduced into *tcm* CLF. A single G116T mutation in the *tcm* CLF yielded >65% octaketide products with an overall polyketide yield comparable to that of wild-type *tcm* KS/CLF. Thus, manipulating one or two residues located at the helix-turn-loop region is sufficient to convert an octaketide synthase into a decaketide synthase, and vice versa. We have shown through rational mutagenesis that CLF exerts polyketide chain length control by defining the size of the polyketide channel, thereby confirming its role as the chain length factor. Residues 109, 112, and 116 in the *act* CLF serve as gatekeepers that terminate the channel at the KS/CLF interface. Reducing the sizes of these residues lengthens the channel and allows two more chain-extending cycles. Our results also suggest that, under *in vivo* conditions, additional proteins that interact with the KS/CLF further bias the formation of polyketides of a particular chain length, highlighting the complexity of protein-protein interactions among the individual type II PKS catalytic units. Our results should lead to novel strategies for the engineered biosynthesis of hitherto unidentified polyketide scaffolds.

The Regio- and Stereo-Specificity of KR

In order to rationally control the reduction pattern of polyketide biosynthesis, we need to understand the structure-function relationship of KR. Towards this goal, we have solved two co-crystal structures of the actinorhodin KR bound with the cofactor $NADP^+$ or NADPH. The crystal structures provide the following information (63):

1. Helices α4-α7 are important for substrate binding.

Analysis of the crystal structure and native gels indicate that KR exists as a tetramer (Figure 5A) (63,64). It has a highly conserved Rossmann fold with the cofactor NADPH bound near the center between two α–β–α motifs and the polyketide substrate bound in a substrate tunnel that opens from the front to the back side (Figure 5B). The front and back sides of KR are defined as the protein face that contains the NADPH binding pocket or be opposite to the NADPH binding pocket, respectively (Figure 5B is the view of the front side). In comparison to fatty acid KRs, the aromatic polyketide KRs contain an extra loop insertion region near α6-α7 (residues 190 – 210, Figure 5B yellow helices). This insertion region is also the most flexible region of KR. Sequence comparison indicates that this insertion region is a unique, highly conserved feature for nine different aromatic polyketide KRs. The regions between α6-α7 and α4-α5 (Fig. 5B, green helices) define the shape of substrate binding pocket and are therefore important for substrate binding.

2. The proton-relay mechanism anchors the substrate by 3-point docking.

Because the cofactor binding pocket and the proposed active site tetrad (Asn114-Ser144-Tyr157-Lys161, Figure 6A) are highly conserved between actinorhodin KR and existing fatty acid KR structures (46,53,54), we can compare the active site geometry and catalytic mechanism by overlapping the structures of actinorhodin KR and fatty acid KRs. We found that the position of the active site tetrad is completely conserved. This indicates that the catalytic mechanism proposed for fatty acid KRs should also apply to polyketide KRs. The catalytic mechanism of the fatty acid KR has been proposed to proceed through a proton-relay network (46,53). Briefly, the ketone substrate is hydrogen bonded to both Ser144 and Tyr157 that constitute the oxyanion hole (Figure 6). Following hydride transfer from NADPH to the ketone substrate, the alkoxide is stabilized by the oxyanion hole while the tyrosyl proton is transferred to the alkoxide (Figure 6B). An extensive proton relay then takes place to replenish the proton extracted from the tyrosyl-OH, sequentially including the 2-OH of NADPH ribose, lysine-NH and then followed by four water molecules (Figure 6B). If this mechanism is correct, then substrate binding is highly restrained by the intricate hydrogen bonding network. The polyketide substrate is docked into the active site using a three-point docking strategy (Figure 6B). Namely, the C9-carbonyl oxygen of the substrate (in purple, Figure 6A) should be hydrogen-bonded with the side chains of Ser144 and Tyr157, while the C9-carbonyl carbon of the substrate should be within hydride-transfer distance to NADPH (Figure 6B).

3. First ring cyclization must occur before ketoreduction to satisfy the C9 regiospecificity.

An important question for aromatic polyketide biosynthesis is the timing of the first ring cyclization, relative to ketoreduction. We found that the timing

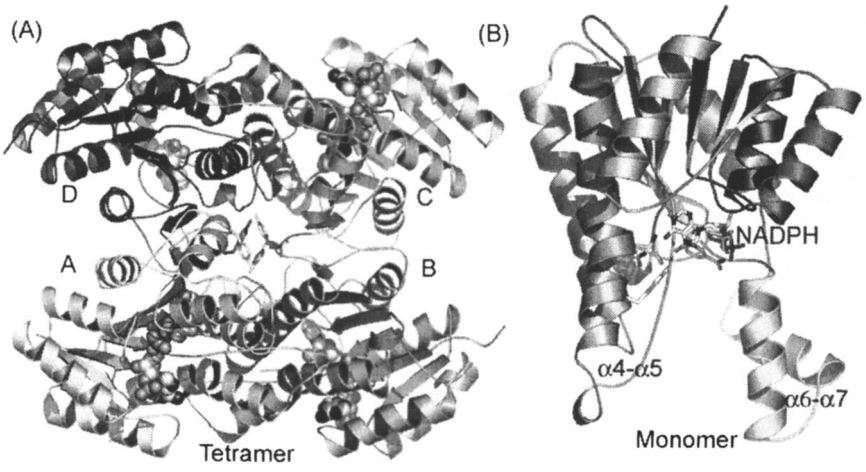

Figure 5. (A) The tetramer model of KR. (B) Enlarged view of the KR monomer

issue is closely related to the C9 regiospecificity. The cyclization of the polyketide chain (producing intermediate **1**, Figure 2) can either occur uncatalyzed, in the active site of KS/CLF, in the interface between KS/CLF, ACP and KR, or in the active site of KR. Substrate docking simulations of the highly flexible linear polyketide chain (intermediate **0**, Figure 2) indicate that it is physically possible to reduce many carbonyl groups of intermediate **0** other than the C9-carbonyl group without evoking protein conformational changes. Due to the flexibility of intermediate **0**, this will result in the loss of the C9 regio-specificity, contradicting results from previous studies that aromatic polyketide KRs are highly specific for C9 reduction. Rather, it is more reasonable to cyclize **0** to **1** prior to the reduction of **1** by KR. Under the dual-constraints imposed by the ring structure of **1** and the three-point docking of the KR active site, the C9-carbonyl group is optimally positioned for ketoreduction when the C7-C12 cyclization takes place (Figure 6B). Similarly, in the case of C5-C10 cyclization, the C7 position (para and meta to the two bulky ring substituents) is selectively reduced. Therefore the cyclization event that leads to **1** is most likely to happen before its reduction by KR.

4. Different binding motifs result in different stereospecificities.

Because of the three-point docking constraint, there are only two possible binding motifs of **1**, either from the front side or the back side of KR. The front side binding motif will lead to the R stereomer, while the back side binding motif will result in the S stereomer (Figure 7). Further, under the dual-constraints

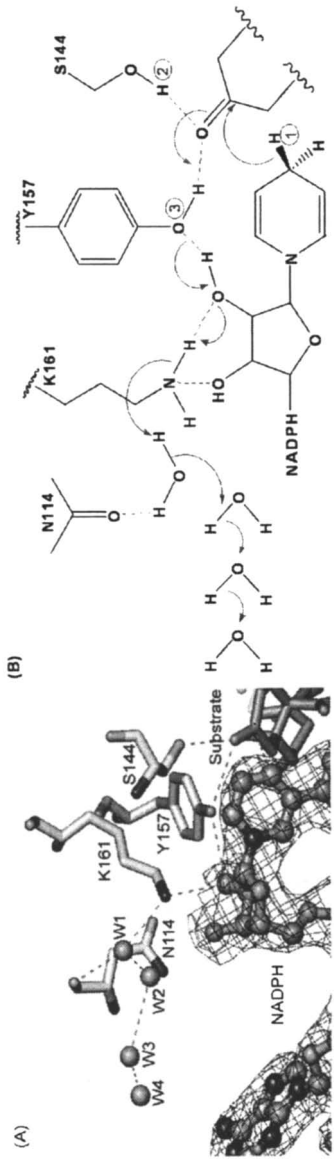

Figure 6. (A) The proton relay network of the actinohodin KR active site. (B) The proposed proton-relay mechanism and the three-point docking of the substrate.

imposed by the ring structure of **1** and the three-point docking of the KR active site, the C9-carbonyl group is optimally positioned for ketoreduction when the C7-C12 cyclization takes place (Figure 2).

The above observations help define the fundamental differences between fatty acid and aromatic polyketide biosynthesis. It is physically possible for fatty acid KR to reduce every carbonyl group of a growing linear polyketide chain (46,53,54). However, for the aromatic polyketide that involves a cyclized polyketide intermediate **1**, it is not energetically favorable for the polyketide KR to reduce carbonyl groups (other than C9) that have an energy penalty imposed by constraints of the active site and substrate geometry. Thus, the first ring cyclization differentiates aromatic PKS from FAS. Finally, sequence comparison indicates that the above features are highly conserved among aromatic polyketide KRs. Therefore mutations of the substrate binding pocket should lead to alternative regio- and stereospecificity for the polyketide substrate. The structures of actinorhodin KR provide an important step toward understanding aromatic polyketide reduction. It also provides the essential base for downstream mutational analyses of its active site and protein surface.

The Cyclization Specificity of ARO/CYC

The aromatic rings are essential for the antibiotic and anticancer activity of polyketides. Understanding the mechanism of aromatic ring formation is crucial for the generation of diverse polyketides with novel or improved therapeutic activity. (27,65). Towards the goal of understanding cyclization specificity, we have crystallized and solved the crystal structure of the tetracenomycin aromatase/cyclase (tcm ARO/CYC) (Figure 8C). Tcm ARO/CYC works directly downstream of tcm KS/CLF to promote the cyclization/aromatization of the first and second rings of tetracenomycin (Figure 1), starting with C9-C14 cyclization (66). Tcm ARO/CYC was cloned from the first 169 residues of the tcmN, a bi-functional enzyme consisting of an N-terminal ARO/CYC domain, and a C-terminal O-methyltransferase domain (66).

The tcm ARO/CYC crystal structure was solved to 1.9 Å using the multiwavelength anomalous diffraction (MAD) method. Our model reveals the following conclusions:

(1) ARO/CYC has a fold that does not resemble any dehydratase fold.

The crystal structure of ARO/CYC consists of seven beta strands, two small alpha helices, and a long C-terminal alpha helix (Figure 8A). This fold resemble the "hot dog in a bun" fold of birch and cherry allergens (67,68). This fold is

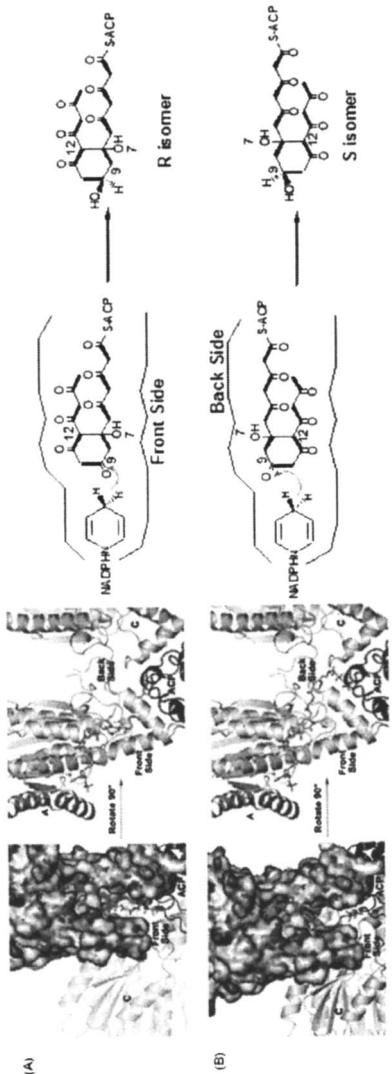

Figure 7. (A) The front side docking results in the R-stereomer during ketoreduction. (B) The back side docking results in the S isomer.

Publication Date: January 11, 2007 | doi: 10.1021/bk-2007-0955.ch012

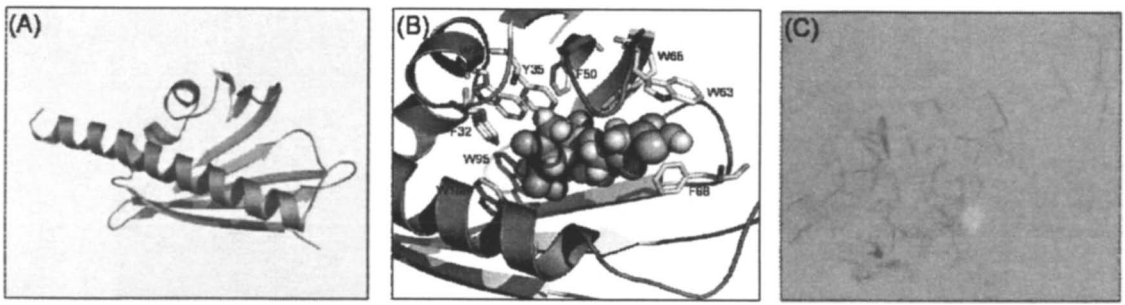

Figure 8. (A) Overall fold of tcm ARO/CYC. (B) Close-up view of binding cavity with a polyketide intermediate docked and hydrophobic aromatic residues labeled. (C) Crystals of ARO/CYC.

In Polyketides; Rimando, Agnes M., et al.;
ACS Symposium Series; American Chemical Society: Washington, DC, 2007.

similar to that of FabZ and scytalone dehydratase, although tcm ARO/CYC has a uniquely deep substrate cavity (Figure 8B, Figure 9) (58,69). Therefore, the crystal structure of the aromatic polyketide ARO/CYC may represent a unique class of dehydratases or cyclases.

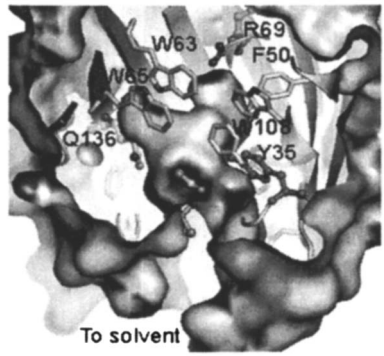

Figure 9. The active site of tcm ARO/CYC

(2) Tcm ARO/CYC has a highly aromatic substrate binding cavity

As shown in Figure 8B, the shape and size of the cavity are defined by many aromatic residues, including Trp28, Trp63, Trp65, Trp95, Trp108, Tyr35, Phe 32, Phe50 and Phe88. The highly aromatic environment will be a strong driving force for aromatic ring formation by stabilizing the transition state of aromatization (Figure 8B, Figure 9).

(3) The active site as a dehydratase

Previously, the crystal structure of a downstream cyclase (tcmI) has been solved. This enzyme cyclizes the fourth ring of tetracenomycin (61). Mutational analysis suggests that tcmI does not actively participate in the chemical reaction. Rather, due to the strong driving force to form the fourth aromatic ring, tcmI serves as a "mold" by steering the auto-cyclization in its substrate-binding cavity (61). TcmI shares no sequence homology with tcm ARO/CYC, and its protein fold is completely different from the tcm ARO/CYC structure. Therefore, tcm ARO/CYC may differ from tcmI by having actual dehydratase function. If this is the case, a general acid or base must be involved. In the active site of tcm ARO/CYC are four semi-conserved hydrophilic residues, Tyr35, Arg69, Gln110, and Asn136, that are identified by substrate docking simulation to serve as the active site base or acid during dehydration . Therefore the dehydration may proceed through a cationic elimination reaction, in which the conserved Arg69 serves as the proton source (Figure 8B, Figure 9).

(4) The molecular basis of ARO/CYC cyclization specificity

Substrate docking also indicates that C9-C14 cyclization is controlled by the size and shape of the binding cavity. Based on sequence alignment between tcm ARO/CYC (a C9-C14 ARO/CYC) and ZhuI (a C7-C12 ARO/CYC), we identified residues that are important to distinguish between these two possible cyclization motifs. For ZhuI, an ARO/CYC that has a C7-C12 cyclization specificity (33), the cavity residues become smaller, such as Tyr28, T35, Asn63, Leu108, Val50 and Val88. The homology model and substrate docking of ZhuI indicates that the polyketide product from C7-C12 cyclization has bulkier substituents than the C9-C14 product, and requires a larger substrate binding cavity. In the future, structure-based mutagenesis will confirm if these cavity residues are indeed important for the cyclization specificity of ARO/CYC.

Concluding Remarks

The structures of KS/CLF, KR and ARO/CYC have provided strong clues to the molecular features that result in the observed chain length, ketoreduction and cyclization specificities during polyketide biosynthesis. Based on structural information, the polyketide chain length has been altered by mutations of the CLF residues at the KS/CLF dimer interface. In the future, it should be possible to mutate residues of KS/CLF, KR and ARO/CYC to change the specificity of ketoreduction and cyclization. Therefore, the crystal structures of PKS domains will serve as the blueprints to guide the combinatorial efforts of polyketide biosynthesis.

Literature Cited

1. Shen, B. *Curr Opin Chem Biol* **2003**, *7*, 285-295.
2. Kim, E.S., Bibb, M.J., Butler, M.J., Hopwood, D.A. & Sherman, D.H. *Gene* **1994**, *141*, 141-142.
3. Motamedi, H. & Hutchinson, C.R. *Proc Natl Acad Sci U S A* **1987**, *84*, 4445-4449.
4. Malpartida, F. & Hopwood, D.A. *Nature* **1984**, *309*, 462-464.
5. Jakobi, K. & Hertweck, C. *J Am Chem Soc* **2004**, *126*, 2298-2299.
6. Otten, S.L., Stutzman-Engwall, K.J. & Hutchinson, C.R. *J Bacteriol* **1990**, *172*, 3427-3434.
7. Blanco, G., Fu, H., Mendez, C., Khosla, C. & Salas, J.A. *Chem Biol* **1996**, *3*, 193-196.
8. Dairi, T., Hamano, Y., Igarashi, Y., Furumai, T. & Oki, T. *Biosci Biotechnol Biochem* **1997**, *61*, 1445-1453.

9. Martin, R., Sterner, O., Alvarez, M.A., de Clercq, E., Bailey, J.E. & Minas, W. *J Antibiot (Tokyo)* **2001**, *54*, 239-249.
10. Li, A. & Piel, J. *Chem Biol* **2002**, *9*, 1017-1026.
11. Khosla, C. & Zawada, R.J. *Trends Biotechnol* **1996**, *14*, 335-341.
12. Woodward, R.B. et al. *Journal of the American Chemical Society* **1981**, *103*, 3210-3213.
13. Woodward, R.B. et al. *Journal of the American Chemical Society* **1981**, *103*, 3213-3215.
14. Woodward, R.B. et al. *Journal of the American Chemical Society* **1981**, *103*, 3215-3217.
15. Pfeifer, B.A., Admiraal, S.J., Gramajo, H., Cane, D.E. & Khosla, C. *Science* **2001**, *291*, 1790-1792.
16. Hopwood, D.A. *Chem Rev* **1997**, *97*, 2465-2498.
17. Hutchinson, C.R. *Chem Rev* **1997**, *97*, 2525-2536.
18. Floss, H.G. *J Ind Microbiol Biotechnol* **2001**, *27*, 183-194.
19. McDaniel, R., Licari, P. & Khosla, C. *Adv Biochem Eng Biotechnol* **2001**, *73*, 31-52.
20. Robinson, J.A. *Philos Trans R Soc Lond B Biol Sci* **1991**, *332*, 107-114.
21. Mendez, C. & Salas, J.A. *Comb Chem High Throughput Screen* **2003**, *6*, 513-526.
22. Bisang, C. et al. *Nature* **1999**, *401*, 502-505.
23. O'Hagan, D. *Nat Prod Rep* **1993**, *10*, 593-624.
24. Meurer, G., Gerlitz, M., Wendt-Pienkowski, E., Vining, L.C., Rohr, J. & Hutchinson, C.R. *Chem Biol* **1997**, *4*, 433-443.
25. Marti, T., Hu, Z., Pohl, N.L., Shah, A.N. & Khosla, C. *J Biol Chem* **2000**, *275*, 33443-33448.
26. Kalaitzis, J.A. & Moore, B.S. *J Nat Prod* **2004**, *67*, 1419-1422.
27. Hertweck, C., Xiang, L., Kalaitzis, J.A., Cheng, Q., Palzer, M. & Moore, B.S. *Chem Biol* **2004**, *11*, 461-468.
28. McDaniel, R., Ebert-Khosla, S., Fu, H., Hopwood, D.A. & Khosla, C. *Proc Natl Acad Sci U S A* **1994**, *91*, 11542-11546.
29. Rix, U., Fischer, C., Remsing, L.L. & Rohr, J. *Nat Prod Rep* **2002**, *19*, 542-580.
30. Kantola, J., Blanco, G., Hautala, A., Kunnari, T., Hakala, J., Mendez, C., Ylihonko, K., Mantsala, P. & Salas, J. *Chem Biol* **1997**, *4*, 751-755.
31. McDaniel, R., Ebert-Khosla, S., Hopwood, D.A. & Khosla, C. *Nature* **1995**, *375*, 549-554.
32. Shen, B. & Hutchinson, C.R. *Proc Natl Acad Sci U S A* **1996**, *93*, 6600-6604.
33. Tang, Y., Lee, T.S. & Khosla, C. *PLoS Biol* **2004**, *2*, E31.
34. Fu, H., McDaniel, R., Hopwood, D.A. & Khosla, C. *Biochemistry* **1994**, *33*, 9321-9326.

35. McDaniel, R., Ebert-Khosla, S., Hopwood, D.A. & Khosla, C. *Science* **1993**, *262*, 1546-1550.
36. Meadows, E.S. & Khosla, C. *Biochemistry* **2001**, *40*, 14855-14861.
37. Carreras, C.W. & Ashley, G.W. *Exs* **2000**, *89*, 89-108.
38. Walsh, C.T. *Science* **2004**, *303*, 1805-1810.
39. Burson, K.K., Huestis, W.H. & Khosla, C. *Abstracts of Papers of the American Chemical Society* **1997**, *213*, 83-Biot.
40. Staunton, J. & Weissman, K.J. *Nat Prod Rep* **2001**, *18*, 380-416.
41. Keatinge-Clay, A.T., Shelat, A.A., Savage, D.F., Tsai, S.C., Miercke, L.J., O'Connell, J.D., 3rd, Khosla, C. & Stroud, R.M. *Structure (Camb)* **2003**, *11*, 147-154.
42. Keatinge-Clay, A.T., Maltby, D.A., Medzihradszky, K.F., Khosla, C. & Stroud, R.M. *Nat Struct Mol Biol* **2004**,
43. Pan, H., Tsai, S., Meadows, E.S., Miercke, L.J., Keatinge-Clay, A.T., O'Connell, J., Khosla, C. & Stroud, R.M. *Structure (Camb)* **2002**, *10*, 1559-1568.
44. Jansson, A., Koskiniemi, H., Erola, A., Wang, J., Mantsala, P., Schneider, G. & Niemi, J. *J Biol Chem* **2004**,
45. Sciara, G., Kendrew, S.G., Miele, A.E., Marsh, N.G., Federici, L., Malatesta, F., Schimperna, G., Savino, C. & Vallone, B. *Embo J* **2003**, *22*, 205-215.
46. Price, A.C., Zhang, Y.M., Rock, C.O. & White, S.W. *Biochemistry* **2001**, *40*, 12772-12781.
47. Huang, W., Jia, J., Edwards, P., Dehesh, K., Schneider, G. & Lindqvist, Y. *Embo J* **1998**, *17*, 1183-1191.
48. Serre, L., Verbree, E.C., Dauter, Z., Stuitje, A.R. & Derewenda, Z.S. *J Biol Chem* **1995**, *270*, 12961-12964.
49. Qiu, X. & Janson, C.A. *Acta Crystallogr D Biol Crystallogr* **2004**, *60*, 1545-1554.
50. Olsen, J.G., Kadziola, A., von Wettstein-Knowles, P., Siggaard-Andersen, M., Lindquist, Y. & Larsen, S. *FEBS Lett* **1999**, *460*, 46-52.
51. Davies, C., Heath, R.J., White, S.W. & Rock, C.O. *Structure Fold Des* **2000**, *8*, 185-195.
52. Price, A.C., Rock, C.O. & White, S.W. *J Bacteriol* **2003**, *185*, 4136-4143.
53. Price, A.C., Zhang, Y.M., Rock, C.O. & White, S.W. *Structure (Camb)* **2004**, *12*, 417-428.
54. Fisher, M., Kroon, J.T., Martindale, W., Stuitje, A.R., Slabas, A.R. & Rafferty, J.B. *Structure Fold Des* **2000**, *8*, 339-347.
55. Rafferty, J.B., Simon, J.W., Baldock, C., Artymiuk, P.J., Baker, P.J., Stuitje, A.R., Slabas, A.R. & Rice, D.W. *Structure* **1995**, *3*, 927-938.
56. Baldock, C., Rafferty, J.B., Stuitje, A.R., Slabas, A.R. & Rice, D.W. *J Mol Biol* **1998**, *284*, 1529-1546.
57. Roujeinikova, A. et al. *J Mol Biol* **1999**, *294*, 527-535.

58. Leesong, M., Henderson, B.S., Gillig, J.R., Schwab, J.M. & Smith, J.L. *Structure* **1996**, *4*, 253-264.
59. Crump, M.P., Crosby, J., Dempsey, C.E., Parkinson, J.A., Murray, M., Hopwood, D.A. & Simpson, T.J. *Biochemistry* **1997**, *36*, 6000-6008.
60. Findlow, S.C., Winsor, C., Simpson, T.J., Crosby, J. & Crump, M.P. *Biochemistry* **2003**, *42*, 8423-8433.
61. Thompson, T.B., Katayama, K., Watanabe, K., Hutchinson, C.R. & Rayment, I. *J Biol Chem* **2004**, *279*, 37956-37963.
62. Sultana, A., Kallio, P., Jansson, A., Wang, J.S., Niemi, J., Mantsala, P. & Schneider, G. *Embo J* **2004**, *23*, 1911-1921.
63. Korman, T.P., Hill, J.A., Vu, T.N. & Tsai, S.C. *Biochemistry* **2004**, *43*, 14529-14538.
64. Hadfield, A.T., Limpkin, C., Teartasin, W., Simpson, T.J., Crosby, J. & Crump, M.P. *Structure (Camb)* **2004**, *12*, 1865-1875.
65. Shen, Y., Yoon, P., Yu, T.W., Floss, H.G., Hopwood, D. & Moore, B.S. *Proc Natl Acad Sci U S A* **1999**, *96*, 3622-3627.
66. Zawada, R.J. & Khosla, C. *J Biol Chem* **1997**, *272*, 16184-16188.
67. Fedorov, A.A., Ball, T., Valenta, R. & Almo, S.C. *Int Arch Allergy Immunol* **1997**, *113*, 109-113.
68. Fedorov, A.A., Ball, T., Mahoney, N.M., Valenta, R. & Almo, S.C. *Structure* **1997**, *5*, 33-45.
69. Wawrzak, Z., Sandalova, T., Steffens, J.J., Basarab, G.S., Lundqvist, T., Lindqvist, Y. & Jordan, D.B. *Proteins* **1999**, *35*, 425-439.